PROTEINS
STRUCTURE ■ FUNCTION ■ BIOINFORMATICS

# Characterization of the AXH domain of Ataxin-1 using enhanced sampling and functional mode analysis

**Marco A. Deriu,[1]* Gianvito Grasso,[1] Jack A. Tuszynski,[2] Diana Massai,[3,4] Diego Gallo,[3] Umberto Morbiducci,[3] and Andrea Danani[1]**

[1] Istituto Dalle Molle Di Studi Sull'intelligenza Artificiale (IDSIA), Scuola Universitaria Professionale Della Svizzera Italiana (SUPSI), Università Della Svizzera Italiana (USI), Centro Galleria 2, Manno, CH-6928, Switzerland

[2] Department of Physics, University of Alberta, Edmonton, Alberta, Canada

[3] Department of Mechanical and Aerospace Engineering, Politecnico Di Torino, Corso Duca Degli Abruzzi 24, Torino, IT-10128, Italy

[4] Department of Cardiothoracic, Transplantation, and Vascular Surgery (HTTG), Leibniz Research Laboratories for Biotechnology and Artificial Organs (LEBAO), Hannover Medical School, Carl-Neuberg-Strabe 1, Hannover, 30625, Germany

**ABSTRACT**

**Ataxin-1 is the protein responsible for the Spinocerebellar ataxia type 1, an incurable neurodegenerative disease caused by polyglutamine expansion. The AXH domain plays a pivotal role in physiological functions of Ataxin-1. In Spinocerebellar ataxia 1, the AXH domain is involved in the misfolding and aggregation pathway. Here molecular modeling is applied to investigate the protein-protein interactions contributing to the AXH dimer stability. Particular attention is focused on: (i) the characterization of AXH monomer-monomer interface; (ii) the molecular description of the AXH monomer-monomer interaction dynamics. Technically, an approach based on functional mode analysis, here applied to replica exchange molecular dynamics trajectories, was employed. The findings of this study are consistent with previous experimental results and elucidate the pivotal role of the I580 residue in mediating the AXH monomer-monomer interaction dynamics.**

Proteins 2016; 84:666–673.


**Key words: neurodegenerative; replica exchange molecular dynamics; Ataxin; functional mode analysis; protein−protein interactions; dimer; AXH; conformational stability.**

## INTRODUCTION

Ataxin-1 is the protein responsible for the Spinocerebellar ataxia type 1 (SCA1), an incurable neurodegenerative disease, related to an anomalous expansion of the polyglutamine (polyQ) tract,[1,2] which leads to the formation of toxic aggregates and neural cellular death.

It has been convincingly demonstrated that protein domains, other than the expanded polyQ tract, are involved in the pathogenesis.[1,3–5] In particular, experimental studies have shown that the AXH domain, a globular region far from the PolyQ tract and responsible for the transcription repression activity, modulates Ataxin-1 misfolding and the aggregation pathway.[6] Similar mechanisms can be observed in other polyQ pathologies such as SCA3, or misfolding-based diseases such as Alzheimer's and Parkinson's. The key role played by the AXH domain in the Ataxin-1 aggregation pathway is borne out by the replacement of the AXH domain with the homologous sequence of the transcription factor HBP1,[6] resulting in a significant reduction of Ataxin-1 aggregation. At the same time, an intrinsic tendency to form fibers, in absence of thermal induction or chemical destabilization, was observed in the isolated AXH.[6]

The AXH domain, the only globular region identified in ATXN1[7] so far, is an unusual chameleon protein

Additional Supporting Information may be found in the online version of this article.

Grant sponsor: Swiss National Supercomputing Centre (CSCS); Grant number: ID S530.

Marco A. Deriu and Gianvito Grasso contributed equally to the work.

*Correspondence to: Marco A. Deriu, Istituto Dalle Molle di studi sull'Intelligenza Artificiale (IDSIA), University for Applied Sciences of Southern Switzerland (SUPSI), Centro Galleria 2, Manno, CH-6928. E-mail: marco.deriu@idsia.ch

Received 22 November 2015; Revised 25 January 2016; Accepted 2 February 2016
Published online 15 February 2016 in Wiley Online Library (wileyonlinelibrary.com). DOI: 10.1002/prot.25017

constituted by an asymmetric homo-dimer,[1] and with an interface characterized by 20-residue motifs mutually adapting, although different.[4] Several experimental studies have identified the AXH dimer as the predominant species in solution,[8] unlike the homologous protein HBP1, which predominantly appears in monomeric form.[3] Despite the well-preserved tertiary and quaternary structure, the N-terminal (Nter) region of each AXH monomer, which is involved in the dimer interface,[7] adopts different topologies leading to asymmetric dimeric interfaces.[4]

Recently, classical and biased molecular dynamics (MD) has been applied to investigate the extensive conformational fluctuation of the Nter tail of the AXH monomer ($AXH^m$) in solution.[9] It has been demonstrated that $AXH^m$ is characterized by a relatively stable structure with, in general, highly conserved domains, except for the Nter tail switching between several conformations.

Based on those findings, and in accordance with previous observations,[7] it has been suggested that interactions leading to the dimer formation might be able to stabilize the Nter region of the $AXH^m$, which is involved in the dimeric interface.[9] However, several issues concerning the protein-protein interactions characterizing AXH conformational stability and, more generally, a dynamic description of protein conformational changes at dimer interface, are still unknown. Computational approaches, and in particular MD, have often demonstrated to be a powerful tool to explore the protein−protein interactions and conformational changes with atomistic resolution.[10–17] In particular, the dimensionality reduction of the trajectory obtained from Replica Exchange Molecular Dynamics (REMD) simulations can be an effective instrument in the identification of the protein-protein dominant binding modes. In this regard, Functional Mode Analysis (FMA) has been recently developed to identify collective atomic motions maximally related to the fluctuation of specific variables of interest.[18]

In this work REMD[19] is applied to investigate protein-protein interactions leading to the AXH dimer stability, focusing on: (i) the characterization of the AXH monomer−monomer interface, and (ii) the molecular description of the monomer-monomer interaction dynamics. A coupled approach, based on FMA applied to REMD trajectories to describe protein conformational changes at the dimer interface, is employed. The findings of the study, in agreement with previous experimental results,[7] demonstrate the pivotal role of the I580 residue in mediating the AXH monomer−monomer interaction dynamics. Finally, the computational results here presented might also be seen as a starting point for further ad hoc experiments focused on evaluating the role of residues here identified in the stability of AXH dimer.

## MATERIALS AND METHODS

### Replica exchange molecular dynamics and mode analysis

The crystal structure of the AXH dimer (PDB code 4APT[7]), already employed in a previous study,[9] was selected here as a starting structure. The 4APT[7] model contains two interacting AXH dimers, AB and CD, (where A, B, C, and D are monomers with identical sequence). For the sake of consistency with the previous literature,[7] residue numbering refers to the UniProtKB/Swiss-Prot entry No. P54253 +1. Each dimer structure AB and CD was placed in a dodecahedron box where the minimum distance between the protein and the edge of the box was set up to 1.2 nm. The box was then fully solvated in explicitly modeled water, and the total charge was neutralized by the addition of $Cl^-$ and $Na^+$ ions. Each system consisted of about 40,000 interacting particles. These systems were first minimized by applying the steepest descent energy minimization algorithm, followed by preliminary position restrained MD of 100 ps (NPT, 1 atm and 310 K) and 50 ps (NVT, 310 K) duration. Then, 128 replicas were generated with temperatures ranging from 300 K to 666 K, and distributed applying the exponential spacing strategy, as previously suggested[20,21] (Supporting Information 1.1). A first NVT position restrained MD was run on each replica for 100 ps. Finally a 50 ns of production NVT-REMD was carried out on each replica at its own temperature, according to previous works.[22–24]

The replicas' exchange interval of 1 ps was considered as being large enough compared to the coupling time of the heat bath ($\tau = 0.1$ ps). The resulting exchange probability was 0.4.

To obtain the canonical average of each physical quantity, the computational data were analyzed as it is usually done in REMD,[23] that is, by time-averaging data over all trajectory steps corresponding to the chosen temperature (in this work 310 K).

As a control, for each AXH dimer, a 500 ns classical MD production run was performed in the NVT ensemble at 310 K.

AMBER99-ILDN force-field[25,26] was used to define the protein topology,[25,27] and the TIP3P model[28] was used to represent the water molecules. The GROMACS 4.6 package was applied for MD simulations and data analysis.[29]

The residues most responsible for monomer-monomer interaction were identified by contact probability plots. Contact probability for each residue was calculated, as reported elsewhere,[30] using the following procedure. For each snapshot extracted from the REMD replica at 310 K, the distance between a residue in one monomer and all residues pertaining to the other monomer was calculated. If at least one distance value, among the

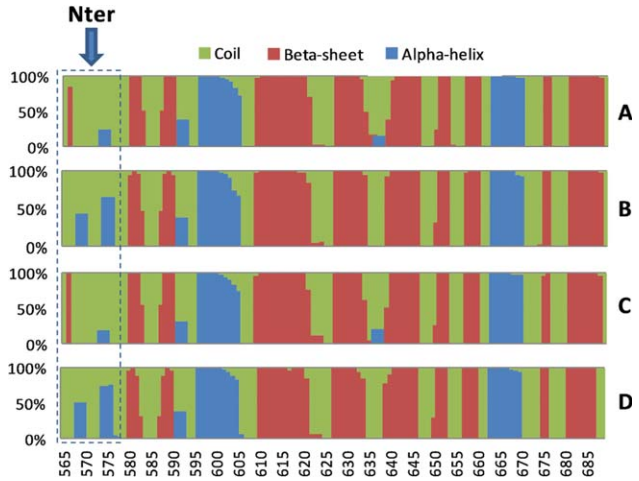


**Figure 1**

Secondary structure probability calculated for each monomer (A,B,C and D) over the REMD trajectory at 310 K in case of AB and CD simulations. The Nter tail is also highlighted.

residue−residue distances, was equal or less than a chosen threshold (0.2 nm), the residue of the first monomer was considered in contact with the interacting one in that snapshot. The number of "contact snapshots" divided by the number of total snapshots taken out from the MD trajectories was defined as the contact probability associated with the residue.[30]

FMA was applied to the REMD trajectory at 310 K to reduce the dimensionality of the system. This allowed the elucidation of collective motions directly related to a specific molecular event.[18] The applied method detects a collective motion maximally correlated to the fluctuation of the quantity of interest, that is, in the case under study the monomer−monomer distance. Assuming that the variable of interest is a linear function of the Principal Components, the maximally correlated vector can be derived by maximizing the Pearson coefficient[18] to quantify the contributions of the individual PCA vectors to the fluctuations of the variables of interest. This approach yields a single collective mode, which drives the phenomenon under investigation, referred to as ensemble-weighted Maximally Correlated Motion (ewMCM).

In applying FMA, it is crucial to cross-validate the derived model for an independent set of simulation frames. The established approach applied for cross-validating the obtained results is to divide the simulation into a subset of frames for model building and a subset of frames for cross-validation. In this work, the obtained maximally correlated motion was validated by predicting the function of interest, in the cross-validation subset, with Pearson correlation coefficient higher than 0.99. Further details of the FMA calculation are provided as Supporting Information S1.2.

## RESULTS

Along the REMD trajectories, the temperature axis was widely explored by each replica and acceptance ratios of more than 0.4 were obtained (Supporting Information S1.1). The computational data were analyzed as time averages over all trajectory steps corresponding to 310K, to study: (i) protein−protein interactions characterizing the AXH dimer, and (ii) protein conformational changes at the dimer interface with atomistic resolution.

More data regarding the structural integrity of the individual monomeric units at 310 K are reported in Supporting Information S1.3.

It is important to remark that the REMD trajectory at 310 K did not sample any dissociation event in AB and CD dimers (Supporting Information Movie 1). Data coming from classical MD simulations on AB and CD systems were in close agreement with the REMD trajectory at 310 K (Supporting Information S1.4).

The dimerization interface in both AB and CD dimers buried 14.5 $nm^2$ of solvent accessible surface. >55% of the contact area is composed of hydrophobic contacts (Supporting Information S1.1). The monomers' secondary structure[30] was evaluated by averaging the 1000 configurations taken from the REMD trajectory at 310K (Fig. 1). It was found that the AXH secondary structure was highly conserved among A, B, C and D monomers,

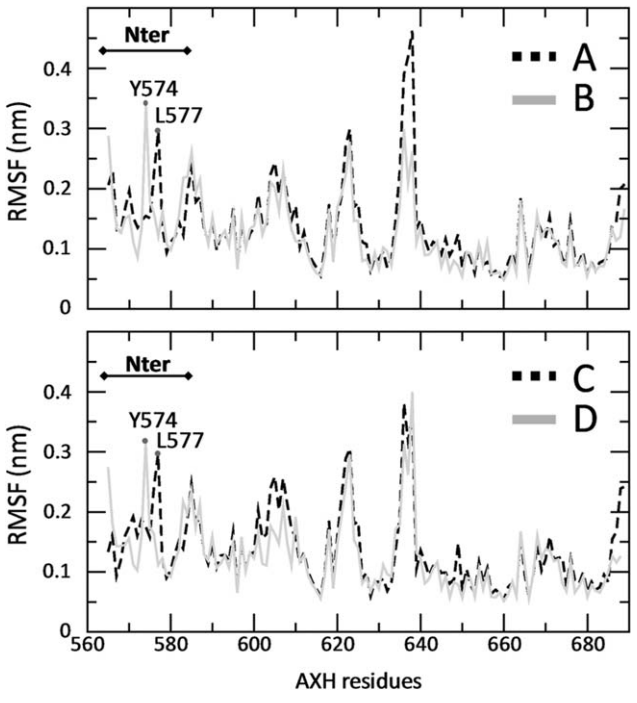


**Figure 2**

Root Mean Square Fluctuation (RMSF) calculated for each monomer (A, B, C and D) over the REMD trajectory at 310 K in case of AB (top) and CD (bottom). The N-ter tail is also highlighted in figure.

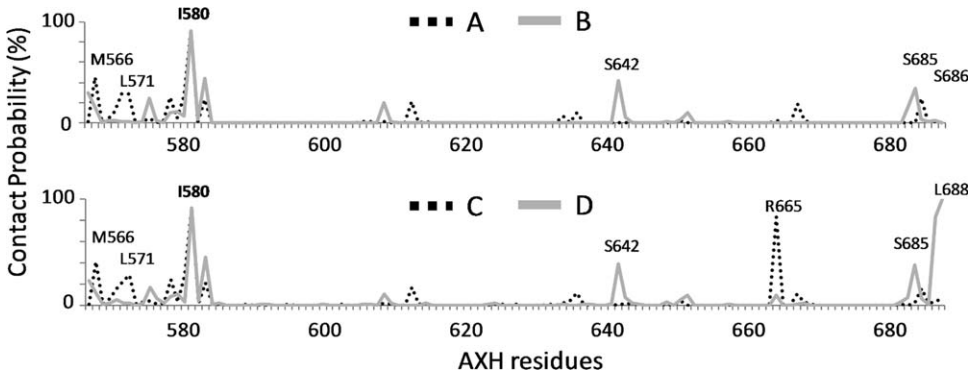


**Figure 3**

AXH inter-monomer contact probability plot calculated for AB and CD dimers by applying a distance cut-off of 0.2 nm. Residues mainly involved in the monomer-monomer contact area are reported in black.

with some exceptions. The main observed differences involve the Nter region, which promotes the asymmetry of the dimerization interface by achieving several different conformations. In agreement with previous investigations,[7] it was found that the protomers B-D differ from A-C, forming a structured helix between residues P568-T570 and P573-F575.

The conformational heterogeneity, or plasticity, of the Nter region also resulted in different Root Mean Square Fluctuation (RMSF) values (Fig. 2). In particular, monomers A and C exhibited higher RMSF values, corresponding to L577 (0.3 nm), with respect to other monomers (0.15 nm). On the contrary, higher fluctuation values (higher than 0.3 nm) for residue Y574 were found in the case of monomer B and D. Another RMSF difference between monomers was located at K638. The cause of the high fluctuation value (0.45 nm) calculated in the case of monomer A was identified in the partial unfolding of the site when compared to other monomers (Fig. 1).

The monomer-monomer residues' contact probability plot is presented in Figure 3. Notably, the dimerization interface was mainly characterized by the interaction between the Nter and C-terminal tails (Fig. 3). Moreover, interacting interfaces were essentially characterized by noncharged residues. In particular I580 is the residue most frequently involved in the AB dimerization interface, being part of the contact area over the 95% of the total sampled configurations. Additional residues M566, L571, S642, S685, and S686 were characterized by lower contact probability values (lower than 50%). In the case of the CD dimer, also R665 and L688 were markedly involved in the dimer interface, as demonstrated by contact probability values of 95% and 98%, respectively.

In view of the already known free energy landscape of the AXH monomer in solution,[9] it is interesting to notice how each Nter conformation sampled for AXH monomers (A, B, C, and D) by REMD at 310K falls in the previously estimated free energy landscape.

It is worth to mention that the free energy landscape of the AXH monomer was calculated in our previous work[9] by applying the Boltzmann Inversion procedure to the probability distribution of the projections along first and second Principal Components taken from the REMD trajectory at 310 K for a single monomer in water[9] (Fig. 4). Black dots in Figure 4 indicate the position on the free energy landscape[9] in term of first and second Principal Components of AHX monomers extracted from the REMD trajectory at 310 K, where monomers are bound in a dimeric form.

Findings presented in Figure 4 describe how monomer A and C conformational state is influenced by the

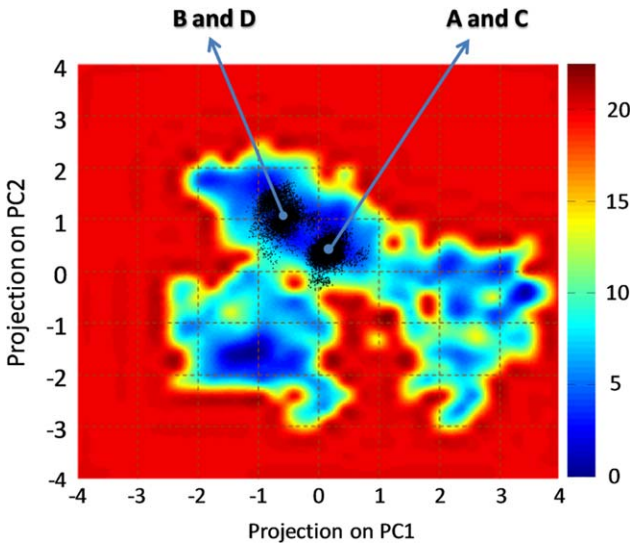


**Figure 4**

Free energy profile (kJ/mol) of the AXH monomer represented as function of the first and second Principal Component projection calculated in our previous work [9]. Labels indicate the position on the free energy landscape in term of first and second Principal Component projection values of the A, B, C and D monomer conformational states sampled in this work along the REMD trajectory at 310K.

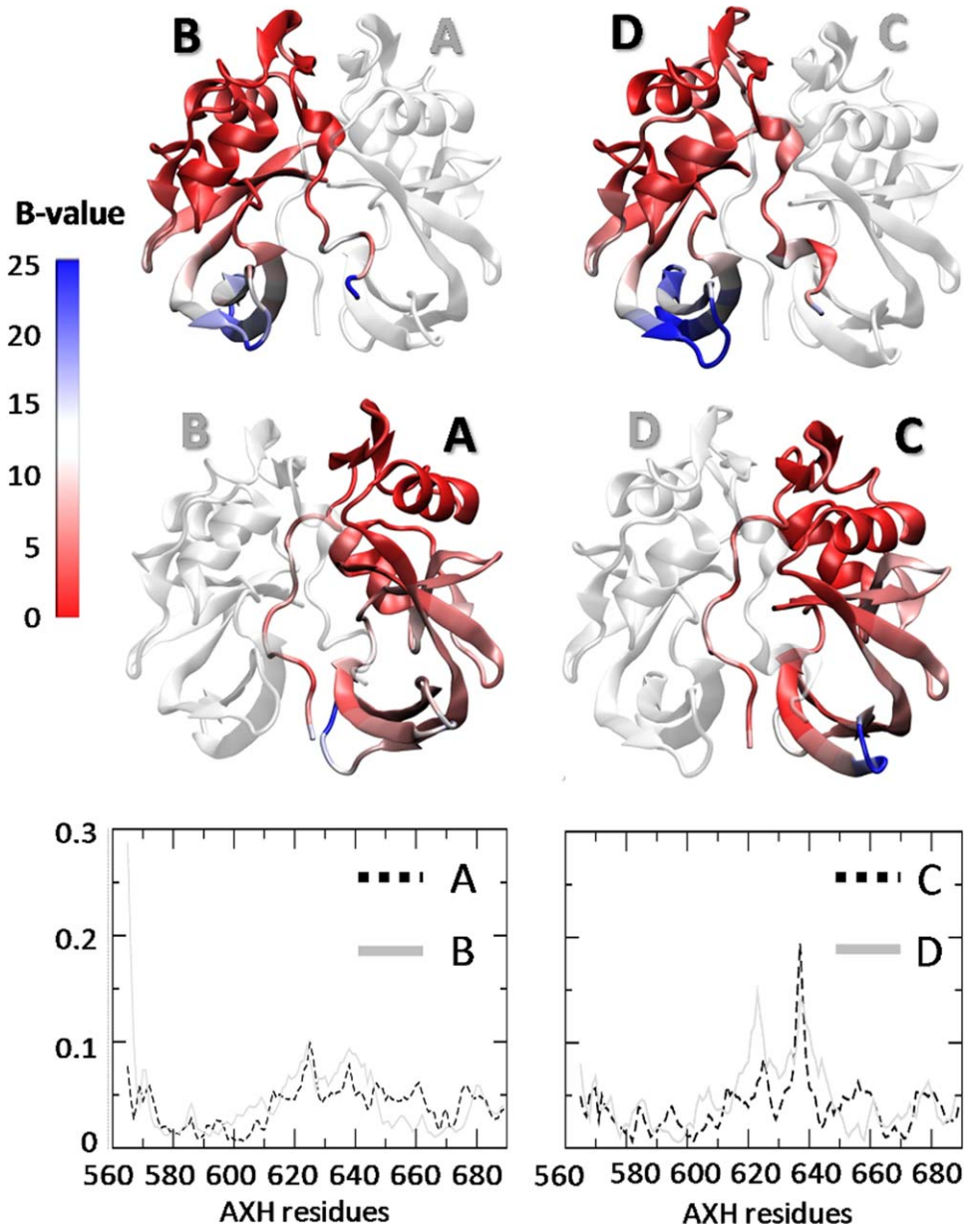


**Figure 5**

Color map of the B-values reported on the AB and CD dimers (top). The B-values are quantified starting from the RMSF plot calculated over the REMD trajectory at 310K filtered on the ewMCM (bottom).

presence of the other interacting monomer B and D, and vice versa. In particular, part of the accessible Nter arrangements previously observed for the AXH monomer,[9] were never observed throughout the AXH dimer dynamics. These findings support the hypothesis that the interactions leading to the dimer formation are able to stabilize the Nter region of the AXH, which is involved in the dimeric interface, as recently proposed.[7,9]

FMA was applied to describe the fluctuation of the inter-monomer distance in terms of internal collective motions of the protein. From FMA it was possible to characterize the contribution of individual PCA vectors to the fluctuations of the monomer−monomer distance, yielding a single vector which drives the monomer−monomer interaction mode, referred to as ewMCM. The analysis of the REMD trajectory at 310 K filtered on the ewMCM, allowed the identification of those residues responsible for the fluctuation of the AB and CD distances (Fig. 5).

In particular, protein domain Q620-P650 was characterized by the highest fluctuation along the filtered trajectory (Fig. 5), suggesting a possible key role in affecting

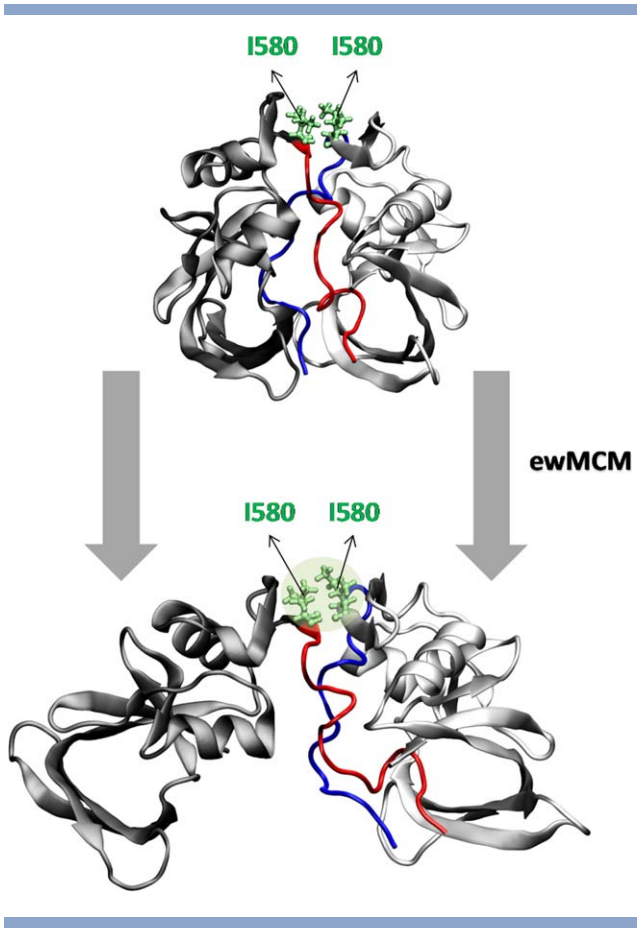


**Figure 6**

Visual inspection of the essential trajectory performed along the ewMCM. The Nter region is highlighted in red (monomer B) and blue (monomer A). Amino acid I580 is highlighted in green. The extension of the motion has been artificially emphasized.

monomer−monomer distance. Also, the Nter tail of monomer A showed high RMSF values. Molecular arrangements of dimers AB and CD are shown in Figure 5, where B-values correspond to the RMSF plot mentioned above. The trajectory filtered on the ewMCM is shown in Figure 6 and Supporting Information Movie 2. To provide a more explanatory visual inspection of the functional motion that makes the inter-monomers distance ($d$) fluctuating within the range $n \times \sigma_d$ (where $\sigma_d$ is the standard deviation of $d$), the extension of the motion was artificially emphasized (Fig. 6 and Supporting Information Movie 3, obtained imposing $n = 6$).

It can be observed that along the monomer-monomer interaction mode, the Nter tail of one monomer (B/D) remains in contact with the other one (A/C). Most importantly, the monomer−monomer interaction mode is far from a simple rigid translation between monomers, exhibiting instead a roto-translational dynamics around a well-defined fulcrum positioned at the Nter basis, where the I580 residues are positioned. The proposed AXH monomer-monomer binding motion confirms the leading role of I580 in affecting the dimer stability as suggested by recent experimental findings.[7]

## DISCUSSION

The present work has been mainly focused on the AXH domain, which is thought to play a key role in the physiological function of the Ataxin-1, and which has been demonstrated to form amyloid fibers *in vitro* without the presence of any destabilizing conditions.[6] The extraordinary structural plasticity, together with the unusual chameleon folding, have made the AXH domain conformational properties the subject of several studies.[1,3–5,8,9,31]

Starting from the assumption that the equilibrium among monomer, dimer and tetramer species of the AXH represents an important point of the aggregation pathway for Ataxin-1,[32] the main aim of this study is to better identify those inter-monomer interactions which are mainly involved in the AXH dimer stability. Results have been obtained by bridging together two approaches: REMD, which provides an enhanced conformational sampling throughout the AHX dimer dynamics, and FMA, which allows dimensionality reduction of the REMD trajectory, thus revealing the motion mode related to the monomer-monomer binding.

Hence, the main novelty of this work resides in the use of molecular simulations and enhanced sampling methods to provide: (i) the characterization of the AXH monomer−monomer interface, and (ii) the molecular description of the AXH monomer−monomer interaction mode.

Supported by very recently estimated AXH monomer free energy landscape,[9] the findings of this study have highlighted how several accessible Nter arrangements, achievable for free AHX monomers in solution, are never observed in the dimeric form. Thus, our findings (1) support the already suggested [7,9] hypothesis that interactions leading to the dimer formation are able to stabilize the Nter region of the AXH, which is involved in the dimeric interface, and (2) confirm that the protein's Nter region is characterized by conformational heterogeneity in terms of its secondary structure (Fig. 1).

In particular, it has been observed that the protomers B-D differ from A-C, and form a structured helix between residues P568-T570 and P573-F575.

Interacting interfaces are essentially characterized by noncharged residues differently from what was observed, for example, for another member of the polyQ family, the Ataxin-3 (ATX3),[30,33] where the Josephin Domain (JD) plays a role in modulating the ATX3 fibrillization pathway. In details, recent investigations[30,33] have indicated that the JD-JD binding might be mainly driven by electrostatic interactions involving charged residues such as Arginine. In the case of AXH dimers, I580 has been

found most frequently involved in the dimerization interface, as being part of the contact area involving over the 95% of the total sampled configurations (Fig. 3).

The key role of I580 is also highlighted by the monomer-monomer interaction mode proposed in this work. The monomer−monomer interaction mode is characterized by a roto-translational dynamics around a well-defined domain including the I580 residue, which acts as a fulcrum. This finding highlights the leading role of I580 in modulating the AXH monomer-monomer interaction, in agreement with a recent experimental study,[7] reporting that the population of the monomeric, dimeric and tetrameric species can be strongly modified by a mutation on I580. Specifically, I580 mutations destabilize the dimer structure, by increasing the monomeric species in the AXH population.[7] Together with the above mentioned pieces of evidence, the results of this work confirm the pivotal role of the I580 residue in stabilizing the AXH dimer.

Finally, additional residues M566, L571, S642, R665, S685 and S686 and L688 were identified here as a potentially important regions involved in the AXH intermonomer interface (Fig. 3). In this connection, the results here presented can be considered as a starting point for further ad hoc experimental and computational studies aimed at validating the direct involvement of these residues in the AXH dimer stability. Moreover, starting from the knowledge of the ewMCM derived from FMA, further investigations are planned and will help in estimating the free energy landscape corresponding to the monomer−monomer dimerization process.

## REFERENCES


1. Chen YW, Allen MD, Veprintsev DB, Löwe J, Bycroft M. The structure of the AXH domain of spinocerebellar ataxin-1. J Biol Chem 2004;279:3758–3765.
2. Zoghbi HY, Orr HT. Pathogenic mechanisms of a polyglutamine-mediated neurodegenerative disease, Spinocerebellar ataxia type 1. J Biol Chem 2009;284:7425–7429.
3. de Chiara C, Giannini C, Adinolfi S, de Boer J, Guida S, Ramos A, Jodice C, Kioussis D, Pastore A. The AXH module: an independently folded domain common to ataxin-1 and HBP1. FEBS Lett 2003;551:107–112.
4. de Chiara C, Menon RP, Adinolfi S, de Boer J, Ktistaki E, Kelly G, Calder L, Kioussis D, Pastore A. The AXH domain adopts alternative folds the solution structure of HBP1 AXH. Structure 2005;13:743–753.
5. de Chiara C, Pastore A. Polyglutamine diseases and neurodegeneration: The example of ataxin-1. In: Brnjas-Kraljević J, Pifat-Mrzljak G, editors. Supramolecular Structure and Function 10. Dordrecht: Springer Netherlands; 2011. pp 87–99.
6. De Chiara C, Menon RP, Dal Piaz F, Calder L, Pastore A. Polyglutamine is not all: the functional role of the AXH domain in the ataxin-1 protein. J Mol Biol 2005;354:883–893.
7. De Chiara C, Rees M, Menon RP, Pauwels K, Lawrence C, Konarev PV, Svergun DI, Martin SR, Chen YW, Pastore A. Self-assembly and conformational heterogeneity of the AXH domain of ataxin-1: an unusual example of a chameleon fold. Biophys J 2013;104:1304–1313.
8. Tsuda H, Jafar-Nejad H, Patel AJ, Sun Y, Chen HK, Rose MF, Venken KJT, Botas J, Orr HT, Bellen HJ, Zoghbi HY. The AXH domain of ataxin-1 mediates neurodegeneration through its interaction with Gfi-1/senseless proteins. Cell 2005;122:633–644.
9. Grasso G, Deriu MA, Tuszynski JA, Gallo D, Morbiducci U, Danani A. Conformational fluctuations of the AXH monomer of Ataxin-1. Proteins Struct Funct Bioinforma 2016;84:52–59.
10. Deriu MA, Grasso G, Tuszynski JA, Gallo D, Morbiducci U, Danani A. Josephin domain structural conformations explored by metadynamics in essential coordinates. PLOS Comput Biol 2016;12:e1004699.
11. Rakers C, Bermudez M, Keller BG, Mortier J, Wolber G. Computational close up on protein-protein interactions: how to unravel the invisible using molecular dynamics simulations? Wiley Interdiscip Rev Comput Mol Sci 2015;5:345–359.
12. Invernizzi G, Lambrughi M, Regonesi ME, Tortora P, Papaleo E. The conformational ensemble of the disordered and aggregation-protective 182-291 region of ataxin-3. Biochim Biophys Acta 2013;1830:5236–5247.
13. Deriu MA, Shkurti A, Paciello G, Bidone TC, Morbiducci U, Ficarra E, Audenino A, Acquaviva A. Multiscale modeling of cellular actin filaments: from atomistic molecular to coarse-grained dynamics. Proteins 2012;80:1598–1609.
14. Deriu MA, Bidone TC, Mastrangelo F, Di Benedetto G, Soncini M, Montevecchi FM, Morbiducci U. Biomechanics of actin filaments: A computational multi-level study. J Biomech 2011;44:630–636.
15. Enemark S, Deriu MA, Soncini M, Redaelli A. Mechanical model of the tubulin dimer based on molecular dynamics simulations. J Biomech Eng 2008;130:041008.
16. Deriu MA, Soncini M, Orsi M, Patel M, Essex JW, Montevecchi FM, Redaelli A. Anisotropic elastic network modeling of entire microtubules. Biophys J 2010;99:2190–2199.
17. Grasso G, Deriu MA, Prat M, Rimondini L, Vernè E, Follenzi A, Danani A. Cell penetrating peptide adsorption on magnetite and silica surfaces: a computational investigation. J Phys Chem B 2015;119:8239–8246.
18. Hub JS, de Groot BL. Detection of functional modes in protein synamics. PLoS Comput Biol 2009;5:e1000480.
19. Sugita Y, Okamoto Y. Replica-exchange molecular dynamics method for protein folding. Chem Phys Lett 1999;314:141–151.
20. Denschlag R, Lingenheil M, Tavan P. Optimal temperature ladders in replica exchange simulations. Chem Phys Lett 2009;473:193–195.
21. Lingenheil M, Denschlag R, Mathias G, Tavan P. Efficiency of exchange schemes in replica exchange. Chem Phys Lett 2009;478:80–84.
22. Zerze GH, Miller CM, Granata D, Mittal J. Free energy surface of an intrinsically disordered protein: comparison between temperature replica exchange molecular dynamics and bias-exchange metadynamics. J Chem Theory Comput 2015;11:2776–2782.
23. Nguyen PH, Stock G, Mittag E, Hu CK, Li MS. Free energy landscape and folding mechanism of a β-hairpin in explicit water: a replica exchange molecular dynamics study. Proteins Struct Funct Genet 2005;61:795–808.
24. Bergonzo C, Henriksen NM, Roe DR, Swails JM, Roitberg AE, Cheatham TE. Multidimensional replica exchange molecular dynamics yields a converged ensemble of an RNA tetranucleotide. J Chem Theory Comput 2014;10:492–499.
25. Hornak V, Abel R, Okur A, Strockbine B, Roitberg A, Simmerling C. Comparison of multiple Amber force fields and development of improved protein backbone parameters. Proteins 2006;65:712–725.
26. Lindorff-Larsen K, Piana S, Palmo K, Maragakis P, Klepeis JL, Dror RO, Shaw DE. Improved side-chain torsion potentials for the Amber ff99SB protein force field. Proteins 2010;78:1950–1958.

27. Lindorff-Larsen K, Maragakis P, Piana S, Eastwood MP, Dror RO, Shaw DE. Systematic validation of protein force fields against experimental data. PLoS One 2012;7:e32131.
28. Jorgensen WL, Chandrasekhar J, Madura JD, Impey RW, Klein ML. Comparison of simple potential functions for simulating liquid water. J Chem Phys 1983;79:926.
29. Hess B, Kutzner C, van der Spoel D, Lindahl E. GROMACS 4: algorithms for highly efficient, load-balanced, and scalable molecular simulation. J Chem Theory Comput 2008;4:435–447.
30. Deriu MA, Grasso G, Licandro G, Danani A, Gallo D, Tuszynski JA, Morbiducci U. Investigation of the josephin domain protein-protein interaction by molecular dynamics. PLoS One 2014;9:e108677.
31. Menon RP, Soong D, de Chiara C, Holt M, McCormick JE, Anilkumar N, Pastore A. Mapping the self-association domains of ataxin-1: identification of novel non overlapping motifs. PeerJ 2014; 2:e323.
32. de Chiara C, Pastore A. Kaleidoscopic protein–protein interactions in the life and death of ataxin-1: new strategies against protein aggregation. Trends Neurosci 2014; 37:211–218.
33. Apicella A, Soncini M, Deriu MA, Natalello A, Bonanomi M, Dellasega D, Tortora P, Regonesi ME, Casari CS. A hydrophobic gold surface triggers misfolding and aggregation of the amyloidogenic Josephin domain in monomeric form, while leaving the oligomers unaffected. PLoS One 2013;8:e58794.